A View on Geometry of Noise Barrier Edges

J. Kokavecz[1], M. Möser[2]
[1] Technische Universität Berlin, Germany, Email: Judith.Kokavecz@TU-Berlin.de
[2] Technische Universität Berlin, Germany, Email: moes0338@mailbox.TU-Berlin.de

Introduction

Noise barriers are a widely spread noise prevention measure. Although a lot of studies spend time on reseaching the edge design, noise barriers are still simple single wall systems in most cases. Because their replacement is not on the list of urban and regional planing, reconstruction might be a cost saving alternative. By using attachments on the edge of existing barriers, their acoustical behaviour could be improved.

The studied attachments are rigid flaps ($Z \to \infty$). In the computer simulations different opening angles for a single flap were tested. To improve the insertion loss a second flap was integrated into the model. The possibilities are numerous with two flaps depending on the opening angles, the length of the flaps and the location of the source. First results for these simulations with different parameter combinations will be shown.

The Model

The model used consists of rigid walls combined into a noise barrier. The first combination includes a simple wall and one flap as attachment (opening angle ϕ_1), the two dimensional profile is shown in Figure 1. The contact point of simple wall and attachment is defined as the point of origin. Along the third dimension the profile is not changing, which is valid for long noise barriers. Therefore a cylindrical coordinate system is used in the model[3][5].

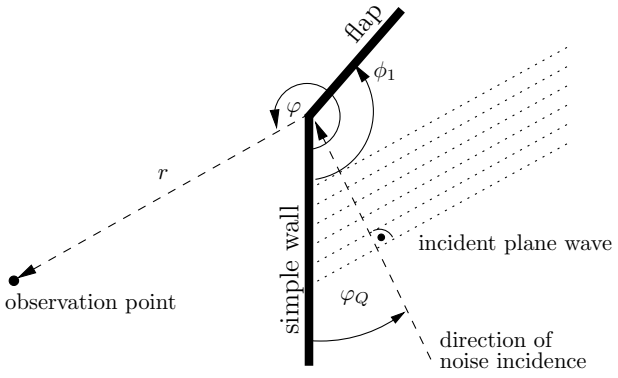

Figure 1: Profile of the model of a noise barrier with one flap as attachment

During the first simulations no ground was included in the model and the simple wall continues from the origin point to infinity. The source is located outside the observation area and represented by an incoming plane wave with the incidence angle φ_Q.

By attaching a second flap to the wall, more variations are possible. First of all one can vary the opening angles of the flaps and then, the flaps length. To cover all these possibilities, a parameter study is necessary and goes beyond the scope of this article.

Numerical Approach

A few more parameters than the ones shown in Figure 1 are needed for the numerical simulation. For an one-flap model the whole area is splitted into three, for a two-flap model into four regions as shown in Figure 2. The first three regions (① - ③) are placed in the circle around the point of origin with radius r_K, which is the flap length. The region ④ is the region outside of this circle. The two opening angles of the flaps are $\phi_1 = \alpha_1$ and $\phi_2 = \alpha_1 + \alpha_2$, the third angle in Figure 2 is $\alpha_3 = 2\pi - \alpha_1 - \alpha_2$.

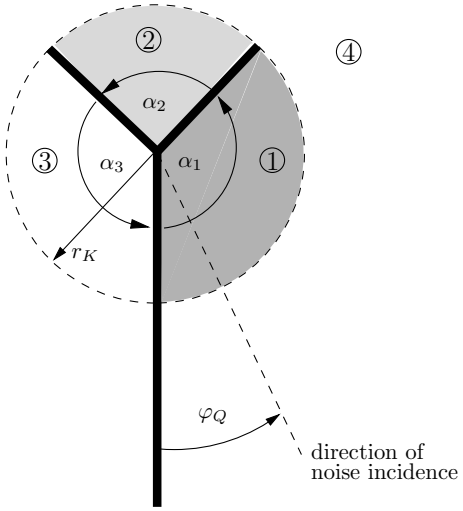

Figure 2: Parameter definition for the numerical simulation

Following the principles in [2] the pressure p in the three inner regions can be calculated by using Bessel functions in the ansatz with the coefficients a_n, b_n and c_n

$$p_1 = \sum_{n=0}^{N_1-1} a_n J_{\frac{n\pi}{\alpha_1}}(kr) \cos\left(\frac{n\pi}{\alpha_1}\varphi\right) \quad (1)$$

$$p_2 = \sum_{n=0}^{N_2-1} b_n J_{\frac{n\pi}{\alpha_2}}(kr) \cos\left(\frac{n\pi}{\alpha_2}(\varphi - \alpha_1)\right) \quad (2)$$

$$p_3 = \sum_{n=0}^{N_3-1} c_n J_{\frac{n\pi}{\alpha_3}}(kr) \cos\left(\frac{n\pi}{\alpha_3}(\varphi - \alpha_1 - \alpha_2)\right) \quad (3)$$

In a numerical simulation only a limited number of points can be included. To avoid aliasing effects, four points per wavelength are used on the circumference, i.e. $N = 4kr_K$ (but a minimum of 20 is used). N_1, N_2 and N_3 are the

number of points in each circular sector. Their ratio is $N_1/\alpha_1 = N_2/\alpha_2 = N_3/\alpha_3$.

In the outer region ④ the pressure is the sum of the pressure caused by the simple wall p_{wall} and the pressure caused by the attachment $p_{\text{attachment}}$

$$p_4 = p_{\text{wall}} + p_{\text{attachment}} \tag{4}$$

The influence of the attachment can be represented by a sum of Hankel functions with the coefficients d_n and the number of points $N = 4kr_K$

$$p_{\text{attachment}}(r,\varphi) = \sum_{n=0}^{N-1} d_n H^{(2)}_{\frac{n}{2}}(kr)\cos\left(\frac{n}{2}\varphi\right) \tag{5}$$

The ansatz for p_{wall} with Bessel functions and the incident plane wave lead to a representation using the Fresnel integrals C and S (see Equations (11) and (12))

$$p_{\text{wall}}(r,\varphi) = p_Q(0)\frac{1+j}{2} \cdot \left(e^{jkr\cos(\varphi-\varphi_0)}\phi_+ + e^{jkr\cos(\varphi+\varphi_0)}\phi_-\right) \tag{6}$$

$$\phi_+ = \frac{1-j}{2} + C\left(\sqrt{2kr}\cos\frac{\varphi-\varphi_Q}{2}\right) - j\,S\left(\sqrt{2kr}\cos\frac{\varphi-\varphi_Q}{2}\right) \tag{7}$$

$$\phi_- = \frac{1-j}{2} + C\left(\sqrt{2kr}\cos\frac{\varphi+\varphi_Q}{2}\right) - j\,S\left(\sqrt{2kr}\cos\frac{\varphi+\varphi_Q}{2}\right) \tag{8}$$

wherein $p_Q(0)$ is the pressure caused by the source at the origin point without any barrier. This term can be used to match the sound level of a realistic source into the simulation.

Calculating the Coefficients

The coefficients a_n, b_n, c_n and d_n can be calculated from the conditions at $r = r_K$. On this circumference there are no sources or drains and therefore the pressure calculated from Equations (1) - (3) is equal to the one calculated from Equation (4)

$$p_4(r=r_K,\varphi) = \begin{cases} p_1(r=r_K,\varphi) & 0 < \varphi \le \alpha_1 \\ p_2(r=r_K,\varphi) & \alpha_1 < \varphi \le \alpha_1+\alpha_2 \\ p_3(r=r_K,\varphi) & \alpha_1+\alpha_2 < \varphi \le 2\pi \end{cases} \tag{9}$$

As second condition, the continuity of the velocity at $r = r_K$ is used

$$v_4(r=r_K,\varphi) = \begin{cases} v_1(r=r_K,\varphi) & 0 < \varphi \le \alpha_1 \\ v_2(r=r_K,\varphi) & \alpha_1 < \varphi \le \alpha_1+\alpha_2 \\ v_3(r=r_K,\varphi) & \alpha_1+\alpha_2 < \varphi \le 2\pi \end{cases} \tag{10}$$

The Farfield Approximation

To (pre-)estimate the effect of the attached flaps one can use a farfield approximation for the pressure. The assumptions made for the observation point in this case are $r \gg r_K$ and $r \gg \lambda$. The first one is easy to realise, it only depends on the flap length. The second one is frequency dependent and determines the lower limit of the observed frequency range. Assuming that the lowest frequency is 30 Hz, the radial distance to the wall must be greater than about 11 m.

In the farfield, the pressure p_{wall} (i.e. the Fresnel integrals) can be approximated by

$$C(x) = \sqrt{\frac{2}{\pi}}\int_0^x \cos(t^2)dt \approx \frac{1}{2} + \frac{1}{\sqrt{2\pi}x}\sin(x^2) \tag{11}$$

$$S(x) = \sqrt{\frac{2}{\pi}}\int_0^x \sin(t^2)dt \approx \frac{1}{2} - \frac{1}{\sqrt{2\pi}x}\cos(x^2) \tag{12}$$

This leads to a simpler description of the pressure field

$$p_{\text{wall}}(r,\varphi) \approx p_Q(0)\frac{(j-1)}{4\sqrt{\pi k}}\frac{e^{-jkr}}{\sqrt{r}} \cdot \left(\frac{1}{\cos\left(\frac{\varphi-\varphi_Q}{2}\right)} + \frac{1}{\cos\left(\frac{\varphi+\varphi_Q}{2}\right)}\right) \tag{13}$$

For $kr \gg N$ i.e. $r \gg r_K$, by using an approximation for the Hankel function[1], the pressure $p_{\text{attachment}}$ becomes

$$p_{\text{attachment}}(r,\varphi) \approx \sqrt{\frac{2}{\pi k}}\,e^{j\frac{\pi}{4}}\frac{e^{-jkr}}{\sqrt{r}}\sum_{n=0}^{\infty} d_n e^{j\frac{n\pi}{4}}\cos\left(\frac{n}{2}\varphi\right) \tag{14}$$

Insertion Loss

To show the improvement due to the attachment, the insertion loss is used. The insertion loss (IL) for the attachment is defined as

$$IL_{\text{attachment}} = 10\lg\left(\frac{|p_{\text{wall}}|^2}{|p_{\text{wall}}+p_{\text{attachment}}|^2}\right) \quad [\text{dB}] \tag{15}$$

For $IL_{\text{attachment}} > 0$ the noise barrier is improved by the attachment.

The farfield approximation (see above) can be used to descibe the improvement by the attachment to be independent of the radial distance between barrier and observation point. This is because of the same dependency of p_{wall} and $p_{\text{attachment}}$ on r. The improvement, represented by the insertion loss depends only on the angle φ in the farfield.

The Results

To get an idea of the effect in the region behind the noise barrier caused by an attachment with $\phi_1 = 120°$, the insertion loss calculated with the farfield approximations

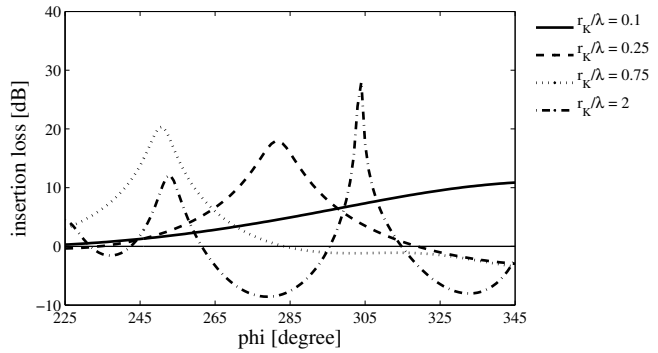

(a) Incidence angle $\varphi_Q = 30°$

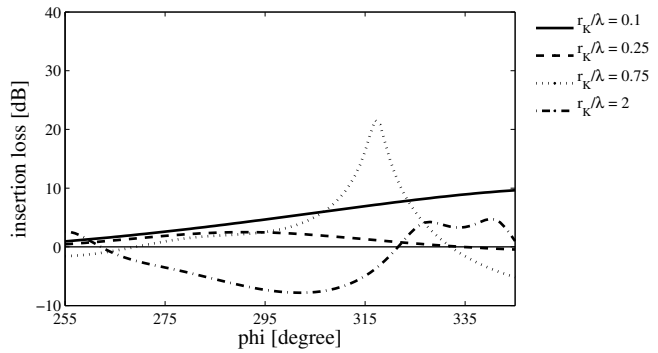

(b) Incidence angle $\varphi_Q = 60°$

Figure 3: Insertion loss plottet over φ, opening angle of the flap $\phi_1 = 120°$

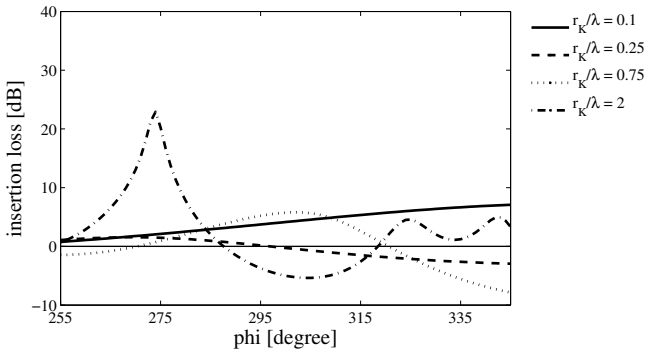

(a) Opening angle of the flap: $\phi_1 = 90°$

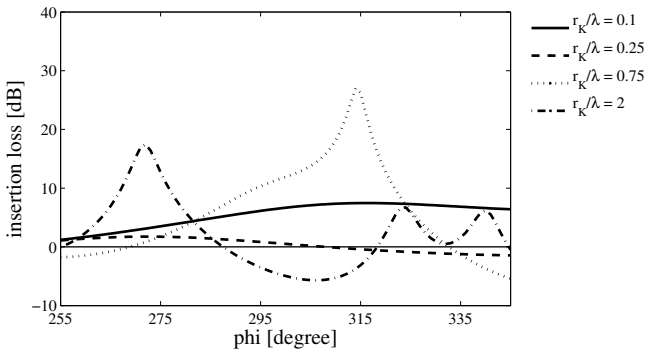

(b) Opening angles of the flaps: $\phi_2 = 90°$ and $\phi_1 = 270°$

Figure 4: Insertion loss plotted over φ, incidence angle $\varphi_Q = 60°$

for the pressure (Equations 13 and 14) is plotted over the angle φ for different r_K/λ ratios and incidence angles of 30° and 60° (shown in Figures 3a and 3b). The insertion loss varies over φ and rises up to 30 dB in narrow regions for $\varphi_Q = 30°$ (Figure 3a). Since diffraction is the mechanism allowing the interference to occur, the smaller the flap, the better the compromise. This means that if the flap is small enough, an overall positive insertion loss is achieved. As the flap grows in size compared to the wavelength, although some high insertion loss peaks are observed, they are to narrow to offer a practical realistic improvement. Besides, those positive peaks are accompanied by even deeper and wider valleys of negative insertion loss. Similar observations can be made for other opening angles.

For an incidend angle of 60° (Figure 3b) the insertion loss has its maximum (20 dB) around $\varphi = 315°$ for $r_K/\lambda = 0.75$. Again an overall improvement can be found for small ratios of r_K/λ. The comparison of Figures 3a and 3b show the influence of the incidence angle φ_Q of the source. The smaller the incidence angle, the higher the insertion loss peaks and the deeper the valleys.

As a result of that, if the goal is an overall general improvement, small flaps seem to be usefull, on the other hand, if a specific region of the space wants to be improved acoustically by the barrier, some specific flap size should accomplish that (disregarding the rest of the space).

The comparison of Figures 3b and 4a shows that the insertion loss depends on the opening angle of the flap. Not only the height of the peaks (and the depth of the valleys) in the insertion loss change with the opening angle, but also the position of these peaks (and valleys).

By adding a second flap, more combinations of opening angles are possible. The difference in the insertion loss between a case with one flap and the same configuration but with a second additional flap is shown in Figures 4a and 4b. In Figure 4a the insertion loss for one flap with an opening angle of 90° is plotted over φ. The second flap has an opening angle of $\phi = 270°$ and the insertion loss reaches higher values for the ratio $r_K/\lambda = 0.75$ (Figure 4b).

Calculating the insertion loss in the farfield approximation is only one possibility to show the effect of an attachment. The problem is that the farfield approximation does not explain what happens around the edge. The insertion loss is caused by the interference between the fronts diffracted at the edges of the noise barrier. This is shown in Figure 5, wherein the blue regions exhibit an improvement due to the flaps, the red ones, a worsening. Near the back of the noise barrier, the highest worsening occurs. Further away an improvement in wide regions is obtained.

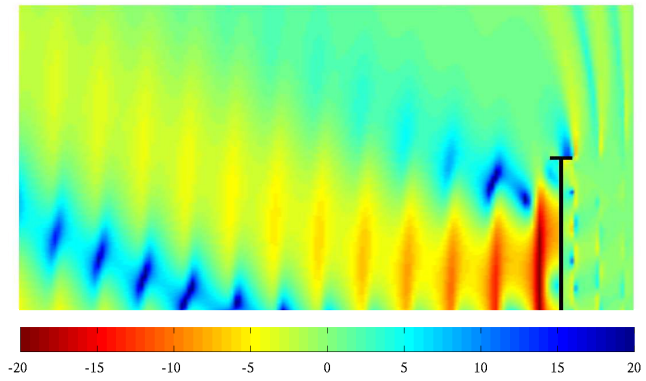

Figure 5: Insertion loss calculated for $r_K/\lambda = 0.75$, $\varphi_Q = 60^\circ$ and opening angles $\phi_1 = 90^\circ$ and $\phi_2 = 270^\circ$

Remarks

In this article a model for noise barriers with flap-like attachments is explained. A possible ansatz for a numerical simulation and first results of this simulation are shown.

The pressure field behind a noise barrier is influenced by its attachment(s). The examples show that attaching a flap or two to a noise barrier improves the screen effect. Because of the huge number of possible combinations of opening angles in the two-flap model, a way to find the optimal one is necessary.

One problem in the model is still the plane wave excitation, which will be replaced by a point source (i.e. a cylindrical source in the three dimensional case) in further studies.

References

[1] M. Abramowitz; I. A. Stegun: Handbook of Mathematical Functions with Formulas, Graphs, and Mathematical Tables. Dover, ninth Dover printing, tenth GPO printing, New York, 1964

[2] Möser, M.: Die Wirkung von zylindrischen Aufsätzen an Schallschirmen. ACUSTICA **81** (1995), 565-586

[3] Möser, M.: Technische Akustik. Springer, Berlin, 2007

[4] Möser, M.; Volz, R.: Improvement of sound barriers using headpieces with finite acoustic impedance. J. Acoust. Soc. Am. (JASA) **106** (1999), 3049-3060

[5] Morse, P. M.; Ingard, K. U.: Theoretical Acoustics. Princeton University Press, 1986

[6] Volz, R.: Schallabweisende Aufsätze zur Verbesserung der Dämmwirkung von Schallschirmen. VDI-Verlag GmbH, Düsseldorf, 2002